Atmos. Chem. Phys. Discuss., 15, 27041–27085, 2015
www.atmos-chem-phys-discuss.net/15/27041/2015/
doi:10.5194/acpd-15-27041-2015

Atmospheric Chemistry and Physics Discussions

Mid-21st century air quality at the urban scale under the influence of changed climate and emissions: case studies for Paris and Stockholm

K. Markakis[1], M. Valari[1], M. Engardt[2], G. Lacressonnière[3], R. Vautard[3], and C. Andersson[2]

[1]Laboratoire de Meteorologie Dynamique, IPSL Laboratoire CEA/CNRS/UVSQ, Ecole Polytechnique, 91128 Palaiseau CEDEX, France
[2]Swedish Meteorological and Hydrological Institute, 60176 Norrköping, Sweden
[3]Laboratoire des Sciences du Climat et de l'Environnement, IPSL Laboratoire CEA/CNRS/UVSQ, Orme des Merisiers, 91191 Gif/Yvette CEDEX, France

Received: 6 July 2015 – Accepted: 8 September 2015 – Published: 7 October 2015

Correspondence to: K. Markakis (konstantinos.markakis@lmd.polytechnique.fr)

Published by Copernicus Publications on behalf of the European Geosciences Union.

Abstract

Ozone, PM_{10} and $PM_{2.5}$ concentrations over Paris, France and Stockholm, Sweden were modeled at 4 and 1 km horizontal resolutions respectively for the present and 2050 periods employing decade-long simulations. We account for large-scale global climate change (RCP-4.5) and fine resolution bottom-up emission projections developed by local experts and quantify their impact on future pollutant concentrations. Moreover, we identify biases related to the implementation of regional scale emission projections over the study areas by comparing modeled pollutant concentrations between the fine and coarse scale simulations. We show that over urban areas with major regional contribution (e.g., the city of Stockholm) the bias due to coarse emission inventory may be significant and lead to policy misclassification. Our results stress the need to better understand the mechanism of bias propagation across the modeling scales in order to design more successful local-scale strategies. We find that the impact of climate change is spatially homogeneous in both regions, implying strong regional influence. The climate benefit for ozone (daily average and maximum) is up to −5 % for Paris and −2 % for Stockholm city. The joined climate benefit on $PM_{2.5}$ and PM_{10} in Paris is between −10 and −5 % while for Stockholm we observe mixed trends up to 3 % depending on season and size class. In Stockholm, emission mitigation leads to concentration reductions up to 15 % for daily average and maximum ozone and 20 % for PM and through a sensitivity analysis we show that this response is entirely due to changes in emissions at the regional scale. On the contrary, over the city of Paris (VOC-limited photochemical regime), local mitigation of NO_x emissions increases future ozone concentrations due to ozone titration inhibition. This competing trend between the respective roles of emission and climate change, results in an increase in 2050 daily average ozone by 2.5 % in Paris. Climate and not emission change appears to be the most influential factor for maximum ozone concentration over the city of Paris, which may be particularly interesting in a health impact perspective.

ACPD
15, 27041–27085, 2015

1 Introduction

There is a growing body of literature on the projected effects of climate and emission reduction scenarios on future air quality. The published research encompass an envelope of models and methodologies; up to now global scale models have been extensively used to study the impact of climate on tropospheric ozone at global or regional scales (Liao et al., 2006; Prather et al., 2003; Szopa and Hauglustaine, 2007), while chemistry transport models (CTMs), having more advanced parameterization of physical and chemical processes, are applied to study selected regions with refined horizontal resolution (Andersson and Engardt, 2010; Colette et al., 2012, 2013; Katragkou et al., 2011; Langner et al., 2012a; Nolte et al., 2008; Zanis et al., 2011).

Numerical models are used to study future evolution of air quality as they allow the evaluation of the effectiveness of planned strategies to mitigate pollutants concentrations. This is particularly important since it is now well established that elevated concentrations deteriorate human health (Jerrett et al., 2009; Lepeule et al., 2012), while new scientific evidence indicate that pollution is harmful at even lower levels than previously thought (REVIHAAP, 2013). There is an increasing number of studies investigating the health effects of population exposure to specific emission source types such as traffic, industry or biomass burning (REVIHAAP, 2013 and references therein). Although a clear association is not established, there is evidence that living near busy roads substantially increases the total burden of disease attributable to air pollution (Pascal et al., 2013). In Europe, one third of the urban population resides in areas where the legislated target value for PM_{10} is exceeded (EEA, 2013).

The fact that today most of the world's (and Europe's) population lives in cities stresses the need to resolve the variability of pollutant concentrations and provide predictions of future air quality at the urban scale (Riahi et al., 2011). Up to now the principal focus of relevant research was solely on the global and regional scales utilizing modeling resolutions of a few hundred (global) to a few tenths (regional) of kilometers. Nevertheless, it has been repeatedly shown that coarse resolutions are inadequate to

ACPD
15, 27041–27085, 2015

resolve fine scale features (Markakis et al., 2014, 2015; Valari and Menut, 2008; Vautard et al., 2007) due to insufficient representation of chemistry and the use of coarse resolution emission inventories that cannot dissociate the strong emission gradients of the large urban agglomerations from those at surrounding rural areas. There is still practically no information on the climate-air quality interactions at the urban and local scales. A reason is the large computational demand in refining model resolution, while maintaining large spatial coverage. Another is the fact that emission scenarios at fine scale are rarely developed, since long-term projections are constrained by the evolution of energy supply and demand, which is a large scale issue. Air quality projections employing locally developed policy are scarce; a first attempt is described in Gidhagen et al. (2012) who developed air quality projections until the near future (2030s) for the greater Stockholm region in Sweden with a high resolution (4 km) modeling system. The impacts were assessed in terms of climate and emissions that were constructed by local experts, however the number of meteorological years included was limited and emissions were projected only for the road transport sector. In Markakis et al. (2014) we describe long-term air quality projections (2050) at urban scale utilizing 10 yr long simulations and fine scale features such as high model resolution (4 km) and an emission inventory developed by local experts for the Il-de-France (IdF; an 8-department area including Paris) region in France.

In the present assessment we implement several improvements compared to the works of Gidhagen et al. (2012) for the Stockholm region and Markakis et al. (2014) for IdF, aiming to improve our knowledge on the climate and pollutants emissions driven air-quality responses at a refined scale. Here we develop a consistent framework including identical climate and emission scenarios at global and regional scales, horizon of projection (2050), number of simulation years (decade) and pollutants considered (ozone, PM_{10} and $PM_{2.5}$). In this work, Stockholm and Paris cities are used as illustrative examples of large urban agglomerations that have very different origins of influence therefore particularly interesting to compare; Paris is largely affected by local emissions while Stockholm experiences significant contribution by non-local sources. We imple-

ACPD
15, 27041–27085, 2015

ment a high resolution modeling grid of 1 km for Stockholm and 4 km for the IdF region. Here (in contrast to Markakis et al., 2014) we take into account changes from large-scale global climate and fine-scale local emissions and disentangle their influence in shaping local concentrations at the 2050 horizon. For Stockholm we additionally quantify the contribution of the locally enforced emission reduction plan from that introduced by the pan-European change in emissions. To describe the future evolution of pollutant emissions at the city scales we rely on high-resolution bottom-up projections at the 2030 horizon developed by local experts (instead of 2020 used in Markakis et al., 2014).

Additionally, we employ the coarse applications that have provided the boundary conditions to the fine scale simulations from which we extract the signal for ozone, PM_{10} and $PM_{2.5}$ future concentration change related to the emission mitigation over the IdF and Stockholm domains. Previous research conducted in IdF (Markakis et al., 2014) indicated a possible overestimation of the ozone concentration response from coarse resolution applications in areas characterized by VOC-limited conditions. More specifically we (Markakis et al., 2014) have identified opposing signals in the projected maximum ozone concentrations, with the regional-scale application to yield large decreases while the urban-scale large increases attributed to the fact that the former implemented top-down coarse resolution emissions and portrayed Paris under NO_x-limited chemistry at present-time conditions, therefore making the city more receptive to forthcoming NO_x emission reductions, compared to the high-resolution simulation portraying a VOC-limited chemistry for Paris. Provided that coarse inventories lack the integration of local policies, this work advances on the work of Markakis et al. (2014) and Gidhagen et al. (2012) by providing the means to identify the differences risen when finer areas are investigated with the refined information of locally developed emission projections and higher resolution. This can help to answer whether there is an added value in integrating local emission-related policy to larger-scale inventories. Specifically for ozone in order to facilitate the comparison between the scales, we examine the long-term evolution of chemical regimes by employing chemical regime

ACPD
15, 27041–27085, 2015

indicators which are a measure of radical production/loss processes (Beekman and Vautard, 2010; Sillman et al., 2003).

2 Materials and methods

The IdF region is located in north-central France (1.25–3.58° E and 47.89–49.45° N) with a population of ca. 11.7 million, more than two million of which live in the city of Paris. The area is situated away from the coast and is characterized by uniform and low topography, not exceeding 200 m a.s.l. Stockholm is located in south-eastern Sweden, with a population of 1.4 million. Stockholm is located partly on islands where the western coast of the Baltic Sea meets Lake Mälaren. Figure 1 illustrates the modeling domains of the urban scale simulations over IdF and Stockholm regions and the boundaries of the cities of Paris and Stockholm. 10 year long simulations were carried out over each domain to represent present-time (1991–2000) and mid-21st century (2046–2055) air quality.

2.1 Regional downscaling of climate and air-quality data

A different chain of models was implemented for each case study. Table 1 summarizes the different models and configurations for the three scales (i.e. global, regional and urban scale) for both meteorology and air quality modeling. To derive projections of the main climate drivers over Europe at 0.11° horizontal resolution (CORDEX coordinated initiative, see Giorgi et al., 2009), we used the IPSL-CM5A-MR (Dufresne et al., 2013) global climate model downscaled with the Weather Research and Forecasting (WRF) regional climate model (Skamarock and Klemp, 2008) for the IdF region and the EC-EARTH global climate model, downscaled with the RCA4 regional climate model (Jacob et al., 2014; Strandberg et al., 2014) for Stockholm. In total, 8 (for present and future) meteorological simulations were implemented in this study.

ACPD
15, 27041–27085, 2015

For both case studies, pollutant concentrations at the global scale were simulated (Szopa et al., 2013) with the LMDz-OR-INCA global model (Hauglustaine et al., 2004) at monthly temporal resolution. The regional downscaling of multi-year pollutant concentration averages though, is done separately for each case study, first over 0.44° (~ 50 km) resolution grids over Europe and then with a single nest over a 4 km resolution grid over the IdF region and a two-step nesting over grids of 0.11° (~ 12 km) and 1 km resolution over Sweden and Stockholm respectively (6 simulations in total were conducted at present day conditions). A thorough presentation of the regional scale air-quality simulations used as boundary conditions for the urban scale runs are provided in Watson et al. (2015).

Two sets of simulations (for each scale) were conducted at future conditions; in the first case we implement future meteorology along with present-time emissions in order to isolate the effect of climate change whereas in the second case we utilize future meteorology and projected emissions to quantify the combined effect of climate and emissions change. The signal of emission mitigation alone can be subsequently derived from the concertation difference between the two aforementioned runs. Finally, only for the Stockholm domain we run an additional test case that allows the quantification of the contribution of emission changes at the regional scale compared to the role of the local scale emission mitigation. This is completed using future projections of local emissions for Stockholm but keeping the respective emissions of the regional scale simulation at present-time levels.

Air-quality simulations were conducted with the CHIMERE (Menut et al., 2013) and MATCH (Robertson et al., 1999) CTMs for the IdF and Stockholm regions respectively. CHIMERE implements is used at both urban and regional scales and it has been benchmarked in a number of model inter-comparison experiments (see Menut et al. (2013) and references therein). The MATCH model is applicable to scales from urban to hemispheric and has been extensively used to study the connection between climate change and air quality in Europe (e.g., Andersson and Engardt, 2010; Engardt et al., 2009; Langner et al., 2005, 2012b). Both models are used operationally for emer-

ACPD
15, 27041–27085, 2015

gency preparedness, environmental surveillance and air-quality forecasts at PREV'AIR (http://www.prevair.org) and SMHI (e.g., http://www.macc.eu) in France and Sweden respectively. The CHIMERE model includes gas-phase, solid-phase and aqueous chemistry, biogenic emission modeling with the MEGAN model (Guenther et al., 2006), dust emissions (Menut et al., 2005) and re-suspension (Vautard et al., 2005) modules. Gas-phase chemistry is based on the MELCHIOR mechanism (Lattuati, 1997) and includes more than 300 reactions of 80 gaseous species. CHIMERE treats sulfates, nitrates, ammonium, organic and black carbon, dust and sea-salt. The gas-particle partitioning is treated with ISORROPIA (Nenes et al., 1998).

The MATCH model includes options for data assimilation (e.g., Kahnert, 2008), modules describing aerosol microphysics (Andersson et al., 2015) and ozone- and particle-forming photo-chemistry considering ~ 60 species (Langner et al., 1998; Andersson et al., 2007, 2015) based on Simpson et al. (2012). MATCH also includes secondary organic aerosol (SOA) formed by oxidation of biogenic and anthropogenic volatile organic compounds (BVOC and AVOC). The SOA-modeling is based on the volatility basis set (VBS) scheme in the EMEP MSC-W model (Bergström et al. (2012) with modifications from Bergström et al., 2014). In the present study, primary organic aerosol emissions were considered non-volatile and VBS schemes were only used for "traditional" ASOA and BSOA; BVOC-emissions of isoprene and monoterpenes (MT) were calculated in the model, using the methodology of Simpson et al. (2012). A small emission of sesquiterpenes, equal to 5 % of the daytime MT emissions, was added (as in Bergström et al., 2014). A detailed description of the organic aerosol scheme in the MATCH model will be presented in a separate publication (Bergström, 2015).

2.2 Urban scale air-quality modeling and emissions

For the urban scale simulations over the IdF region we used the same model setup as in Markakis et al. (2014, 2015) with a mesh-grid of 4 km horizontal resolution consisting of 39 grid cells in the west–east direction and 32 grid cells in the north–south direction. Based on the sensitivity on vertical model resolution presented in Markakis et al. (2015)

ACPD
15, 27041–27085, 2015

we structure the model with a relatively coarse resolution of 8 σ-p hybrid vertical layers from the surface (999 hPa) up to 5.5 km (500 hPa). The lowest layer is 25 m thick. The 1 km resolution domain, covering Stockholm, consists of 48 × 48 grid cells. The vertical resolution follows the layers of the driving RCM, distributed between 20 layers with a 60 m thick surface layer.

Present-time emission estimates for the IdF region are available at a 1 km resolution grid. Emissions are compiled with a bottom-up approach by the IdF environmental agency (AIRPARIF) combining a plethora of city-specific information (AIRPARIF, 2012). The spatial allocation of emissions is either source specific (e.g. locations of point sources) or completed with proxies such as high-resolution population maps and a detailed road network. The inventory has hourly source specific, temporal resolution. The compilation of present-time emission for the Stockholm region (covering an area of 30 municipalities and ca. 2 million inhabitants) is also based on a bottom-up approach e.g., the estimates of total traffic volumes are primarily based on in-situ measurements and variations of vehicle composition and temporal variation of the traffic volumes are described for different road types. Vehicle fleet composition and vehicle exhaust emission factors are based on the Swedish application of the ARTEMIS model (Sjödin et al., 2006). There are also large non-tailpipe emissions due to road, tyre and break wear. In Stockholm the non-tailpipe emissions dominate and emission factors are estimated based on local measurements (Omstedt et al., 2005; Ketzel et al., 2007). The emission database has hourly source specific, temporal resolution. More details on the emission data and how they were compiled can be found in Gidhagen et al. (2012).

2.3 Climate and regional scale emission projections

Climate follows the long-term RCP-4.5 pathway that exhibits a 20 % greenhouse gas emission reduction for Europe, constant population and mid-21st century global radiative forcing at 4 W m^{-2}, increasing to 4.5 W m^{-2} by 2065 and stabilizing thereafter (Clarke et al., 2007). Shown in previous work (Markakis et al., 2014) this scenario represents an intermediate alternative between the pessimistic and optimistic RCPs (8.5

ACPD
15, 27041–27085, 2015

and 2.6 respectively) in terms of long-term temperature projection in IdF with 0.6 °C increase in the 2050 annual average temperature compared to −0.5 °C for RCP-2.6 and +1.1 °C for RCP-8.5.

The European scale simulations use anthropogenic emissions developed in the framework of the "Evaluating the Climate and Air Quality Impacts of Short-Lived Pollutants" (ECLIPSE) project (Klimont et al., 2013). The ECLIPSE inventory implements emission factors from the GAINS model (Amann et al., 2011) and it is consistent with the long-term climate projections of the RCPs but also includes spatial algorithms to improve the representation of short-term continental and national air quality legislations. In this study we used the "Current Legislation Emission" scenario (CLE) for mid-21st century in Europe, which includes both climate and regional air quality policies and assumes full enforcement of all legislated control technologies until 2030 and no climate policy thereafter. CLE projects that NO_x, NMVOCs, PM_{10} and $PM_{2.5}$ emissions drop in 2050 by 43, 35, 32 and 32 % respectively compared to the present day. The MATCH simulations include biomass burning emissions as well taken from the Atmospheric Chemistry and Climate Model Intercomparison Project (ACCMIP) database (Lamarque et al., 2010).

Urban-scale emission projections

The IdF region with the support of the "Direction Regionale et Interdepartementale de l'Environnement et de l'Energie d'Ile de France" (DRIEE-IF), has introduced the "Plan de Protection de l'Atmosphere d'Ile de France" (PPA) enforcing short and long term emission cutbacks in order to comply with the national legislation of air pollution concentration reductions. The 2030 emission projection for the IdF region includes gradual renewal of the vehicle fleet to Euro VI, increased use of public transport, replacement of domestic fuel for heating with electricity and gas, new French thermal regulations in buildings, aviation traffic projections and implementation of planned legislation for the industrial sector. The emission projection for the county of Stockholm is founded on vehicle fleet evolution and emission factors for 2030 based on the application of the

ACPD
15, 27041–27085, 2015

ARTEMIS model (details found in Gidhagen et al., 2012). Other emissions besides the traffic-related were not changed from the present to the future in Stockholm.

Figure 2 illustrates the annual, sectoral emissions of NO_x, NMVOCs, PM_{10} and $PM_{2.5}$ in the IdF domain for the present-time and the 2030 scenario. Present-time NO_x emissions mainly stem from the transport sector (~ 60 % of annual emissions), largely mitigated by 2030 (emissions decline from 60 to 20 Gg). The leading emitter of NMVOCs at present-time is the "use of solvents" sector accounting for 49 % of all-sector annual emissions. Interestingly the emissions coming from this sector are hardly mitigated in the future compared to NO_x; the corresponding reduction reaches only 11 %. The transport, industrial and heating sectors have important PM_{10} emission shares at present day. The heating and transport sectors are strongly mitigated (reductions reach ~ 60 %) while industrial emissions are abated by only 18 % mainly due to the fact that their primary origin is fugitive dust released during production processes whereas the mitigation plan introduces fuel-based reductions. The main contributors of annual fine particles emissions are the transport and the heating sectors, both strongly mitigated strongly by 2030 (transport sector's emissions drop by 96 %). Total present-time emissions are reduced by 55 % for NO_x, 32 % for NMVOCs, 37 % for PM_{10} and 54 % for $PM_{2.5}$. For Stockholm the domain-wide NO_x, NMVOCs and primary PM_{10} emissions decrease by 16, 18 and 10 % respectively. The decrease in emissions is mainly a result of planned renewal of the traffic fleet and stricter emission limits.

Finally, we assume that local emissions are unchanged between 2030 and 2050 to be in line with the larger-scale perspective; the European scale emissions in the same period decrease by only 3.4 % for NO_x, 1.2 % for NMVOCs, 1 % for PM_{10} and 1 % for $PM_{2.5}$.

3 Model evaluation

In this section we evaluate the present day simulations at the study domains. Surface ozone concentrations modeled with CHIMERE and MATCH (averaged over the ozone

ACPD
15, 27041–27085, 2015

period which spans from April to August) were compared against measurements of the air-quality networks of the cities e.g., 17 urban, 5 suburban and 8 rural sites in IdF and one urban site (Torkel Knutsson) in Stockholm. We also evaluate maximum ozone concentrations calculated from 8 h running means (MD8hr). Modeled PM_{10} and $PM_{2.5}$ ground-level concentrations in summer (JJA), winter (DJF) and on annual basis are compared to 7 urban stations in IdF and 1 station in the Stockholm region. Results are illustrated with scatter plots in Fig. 3. For Stockholm we additionally evaluate the organic carbon (OC) and elemental carbon (EC) as well as salt (as sodium) using measurements conducted during the years 2002–2003 and 2013 respectively at the remote site of Aspvreten.

Figure 3a shows that over the urban stations of IdF, CHIMERE overestimates daily ozone (overall bias = 10 %) mostly at the sites outside the city center; focusing on monitoring sites inside Paris the model bias is only 3.7 % (not shown). The simulation successfully reproduces MD8hr. Overestimation of daily ozone is observed at suburban (+14.6 %) and rural (+13.3 %) stations. Discrepancies in rural ozone may be due to overproduction of isoprene emissions due to a warm modelled bias (+0.3°, not shown) or enhanced advection from the boundaries.

The evaluation of $PM_{2.5}$ in Paris (Fig. 3b) shows a negligible mean bias during winter but overestimation by +15.3 % in the summer. Simulations in Markakis et al. (2014), where dust emissions were not included, showed an underestimation of both summer and winter concentrations suggesting that CHIMERE might overproduce dust particles especially in the drier summer period. While this exaggeration is also valid for PM_{10}, summertime concentrations in Paris are generally well represented (Fig. 3c). It is possible that the stronger modeled winds in winter compared to observations (not shown) affect the larger particles more, through accelerated dry deposition (Megaritis et al., 2014).

For the Stockholm case we have first identified the regional and local contributions of emissions to ozone, PM_{10} and $PM_{2.5}$ concentrations utilizing measurements from the rural site of Norr Malma (results are tabulated in Table 2). This site, located 80 km

ACPD
15, 27041–27085, 2015

north-east of Stockholm, is only slightly affected by urban plumes, therefore we use it as an indicator of the regional influence in the area. The local contribution is defined as the difference between concentrations monitored at the Torkel Knutsson (urban) and Norr Malma (rural) sites. The Stockholm city exhibits weak titration as the daily average ozone concentrations measured at the two sites are similar (Table 2). The performance of MATCH is therefore mainly driven by the simulations at the coarser scales which overestimate nighttime ozone (not shown) due to too efficient vertical mixing during the night; this results for the MATCH model to overestimate the regional contribution in Stockholm by 17 % (not shown), which also explains the major part of the positive bias at the 1 km resolution simulation by 10 % (Fig. 3d). On the contrary, the regional contribution in modeled MD8hr is well represented (bias < 1 %) leading to unbiased MD8hr in the high-resolution modeling.

Annual mean $PM_{2.5}$ concentrations are accurately reproduced (Fig. 3e) by the MATCH model over the city but summertime levels are overestimated by 14 % and wintertime by 40 %. This is due to a large over-production in total sea salt in the Stockholm domain, during the whole year (+2.1 $\mu g\,m^{-3}$), but mostly during winter (+3 $\mu g\,m^{-3}$). Despite this an underestimation of PM_{10} concentrations by 26 % is observed over the whole year (Fig. 3f). This is due to a large summertime underprediction of PM_{10} (40 %), partly explained by the model's lack of aerosols of biogenic origin, which are mainly assigned to the coarse mode of the size distribution. Spores and other primary organic material have an important contribution to the speciation of the organic aerosol in northern Europe (20 to 32 % of the total carbon during summer, Yttri et al., 2011). Another possible reason is the underestimation of OC (by 1.5 $\mu g\,m^{-3}$) and EC (by 0.1 $\mu g\,m^{-3}$), which is probably due to the bias inherited by the regional scale simulations since less than 38 and 26 % of city's PM_{10} and $PM_{2.5}$ concentrations respectively stem from local sources (Table 2). The regional contribution to PM_{10} concentrations based on monitor data is about 60 % but due to the aforementioned reasons 17 % lower based on the MATCH simulation (annual average) mainly stemming from the summer period (−43 %).

ACPD
15, 27041–27085, 2015

4 Present-time air-quality modeling analysis

Maps of present-time ozone daily average concentrations (in the ozone period) and annual mean PM_{10} and $PM_{2.5}$ concentrations are illustrated in the left columns of Figs. 4 and 5 for IdF and Stockholm domain respectively. Concentrations that are spatially averaged over the cities of Paris and Stockholm (see Fig. 1) and domain-averaged concentrations that are representative of rural areas, are discussed separately. Consequently, lower ozone concentrations are found over the city-centers due to titration while higher levels are modeled at the surrounding areas due to photochemical formation (IdF) or long-range transport (Stockholm). The urban increment of daily average ozone, defined here as the difference between the urban and the domain-averaged concentration, is $-13\,\mu g\,m^{-3}$ in IdF and only $-1\,\mu g\,m^{-3}$ in the Stockholm domain. Ozone formation in IdF is VOC-limited and therefore, titration rate over Paris is high (Markakis et al., 2014). On the contrary, ozone levels over the city of Stockholm are mainly due to transport from the boundaries and much less affected by local NO_x emission and titration (see also discussion in the previous section). Annual $PM_{2.5}$ and PM_{10} concentrations (Fig. 4e and i) are high over areas of intense anthropogenic activity such as the Charles-de-Gaulle international airport (north-east in the IdF domain), the city-centre and the suburbs of Paris due to road transport and wintertime heating emissions while local dust contributes with PM_{10} emissions to the south. The spatial pattern of $PM_{2.5}$ and PM_{10} concentrations in the Stockholm domain mainly reflects major roads, i.e. traffic emissions (Fig. 4e and i).

5 Future climate and air-quality analysis

5.1 Climate projections for 2050

In Table 3 we show the projected domain-wide values of key meteorological variables. A warmer climate is expected in both regions. Surface temperature in IdF increases

ACPD
15, 27041–27085, 2015

by 0.2 °C in summer and 0.4 °C in winter while in the Stockholm domain this trend is stronger reaching +1.3 °C in summer and +1.4 °C in winter. During the summer months, when ozone formation mainly occurs, no significant change in solar radiation is observed. Ground-level wintertime specific humidity rises by ∼ 6 % in IdF and by +7 and +9.7 % in summer and winter respectively over Stockholm. The effect of humidity on ozone levels is ambiguous (see Jacob and Winner (2009) for a thorough discussion); elevated levels are linked with lower levels of background ozone (Johnson et al., 1999) even though some have found a weak effect in more polluted atmospheres (Aw and Kleeman, 2003). Changes in the planetary boundary layer height (PBL) affect pollutants dispersion. In IdF we observe an increase by 3.4 % in PBL during the summer and decrease by 5.6 % during winter. In the Stockholm domain projected changes in the PBL are less than 2 %.

The precipitation rate, a regulating factor of PM concentrations, increase by 6.5 and 3.6 % during summer and winter respectively in IdF whereas, summertime precipitation in the Stockholm domain decreases by 6.3 % and wintertime levels increase by only 1.7 %. Nitrate concentrations are expected to increase with humidity due to shift of the ammonia-nitric acid equilibrium to the aerosol phase (Seinfeld and Pandis, 2006) but to decrease due to the higher temperatures. On the other hand, sulfates increase with the warmer climate while there is evidence that elevated humidity may also lead to decrease in particle concentration by increasing the water content of particles and accelerating dry deposition rates (Megaritis et al., 2014). A warmer climate may also affect secondary organic production since semi-volatile pollutants are more prone to the gas phase under warm temperatures. Furthermore, climate change induced changes to the oxidizing capacity may cause changes to the volatility of organic gases.

5.2 Local air quality at 2050 due to climate change

Figures 4 and 5 show the future changes (compared to present-time) in daily ozone daily concentrations (averaged in the ozone period) and annual mean PM_{10} and $PM_{2.5}$ concentrations, due (i) only to climate change, (ii) only to emission reductions and (iii) to

ACPD
15, 27041–27085, 2015

the combined effect of climate and emissions for IdF and Stockholm regions respectively. The spatial distribution of the ozone concentration difference (daily and MD8hr) between present and future reveal that despite the overall increase of mean surface temperature there is a domain-wide climate benefit for both domains (Table 4). In Paris reductions in the daily and MD8hr ozone concentrations reach ∼ 5 %. To some extent this is explained by the locale climate change; decrease in surface ozone despite the warmer climate has been also observed by other researchers (Coleman et al., 2014; Fiore et al., 2005; Lauwaet et al., 2014) and linked with enhanced ozone destruction through the $O_3 + OH \rightarrow HO_2 + O_2$ reaction due to increase in OH radicals triggered by higher surface water vapour ($O(^1D) + H_2O \rightarrow 2OH$). For Paris this is consistent with the fact that NO_x concentrations are not much affected in the future ($\Delta c = 1.2\,\mu g\,m^{-3}$) and therefore the decrease in ozone cannot be attributed to enhanced titration. The increase of the summertime period PBL height could also be responsible for the declining ozone trends through less dispersed primary NO_x emissions. Most probably changes in regional climate are responsible for the observed trend e.g., a weakened outflow from North America which is known to affect Europe through the north and western boundaries (Auvray and Bey, 2005; Lacressonnière et al., 2014). This is consistent with the fact that Paris and the IdF average responses are equivalent (Table 4) also evident in the Stockholm case which is known to have significant regional influence. Overall ozone concentration response in the Stockholm domain is negligible (∼ 2 % for daily average and MD8hr ozone) driven by the respective response at the regional level (Watson et al., 2015).

Changes in future concentrations of particles in IdF are up to 5 and 10 % for PM_{10} and $PM_{2.5}$ respectively, depending on season and area of focus (Paris or IdF average, Table 4). There is a weak climate benefit for annual concentrations of PM over Paris and the domain, mainly due to enhanced summertime precipitation. A small increase in PM concentrations over Paris is observed in wintertime as a result of a shallower boundary layer and higher temperatures that positively affect sulfates. PM annual concentrations over the Stockholm domain remain practically unchanged; a weak decrease of 3 %

ACPD
15, 27041–27085, 2015

is only estimated during winter, and similarly to ozone it is linked to regional-scale changes.

5.3 Local air quality at 2050 due to emission reductions

The spatial distribution of changes in annual average ozone concentrations due to emission mitigation in the IdF region reveals two opposing trends (Fig. 4c); in Paris there is an overall increase of daily ozone by 4.8 $\mu g\,m^{-3}$ (Table 4) despite the enforced NO_x emission mitigation. Under the VOC-limited photochemical regime characterizing the city, NO_x abatement inhibits the ozone titration process resulting in higher ozone levels. The magnitude of the ozone increase due to emission mitigation outbalances the predicted climate benefit and the combined effect leads to an overall penalty of +1.5 $\mu g\,m^{-3}$ over Paris. In contrast, the domain-wide ozone concentrations decrease by 6.5 $\mu g\,m^{-3}$ since ozone over the rural areas are less affected by titration (Markakis et al., 2014). It is worth noting that the absolute change in the MD8hr concentration over Paris due to climate change is two times higher than due to emission mitigation (Table 4). Therefore, while local emission mitigation has a stronger impact on background ozone levels, climate change affects more the ozone peaks (found at around 15:00 LT in Paris). This may be particularly interesting from a health impact assessment standpoint where the MD8hr indicator is typically implemented (Likhvar et al., 2015).

Emission reduction policies appear to be more efficient for ozone abatement over the Stockholm region, with reductions reaching ~ 11 and $\sim 13\,\mu g\,m^{-3}$ for the average and MD8hr respectively indistinctively for the city and the domain-averaged concentrations (Table 4). Based on the sensitivity simulations we find that the observed ozone decrease is entirely attributed to emission mitigation at the regional rather than the local scale (Table 5). We should note however, that the role of local emission reductions is probably underestimated in Stockholm due to lack of non-traffic emission abatement.

Particle concentrations are very sensitive to their primary emission changes (Markakis et al., 2015). Therefore, it is not surprising that PM concentration reductions are mainly due to emission mitigation in both domains (Table 4). The domain-wide an-

ACPD
15, 27041–27085, 2015

nual average in IdF decline by 7.2 and 8.1 $\mu g\,m^{-3}$ and in the Stockholm domain by 1.9 and 1.6 $\mu g\,m^{-3}$ for PM_{10} and $PM_{2.5}$ respectively. In IdF the decrease is higher over areas and seasons with high primary PM, e.g., Paris compared to the rural areas of IdF (Fig. 4g and k) as well as in wintertime compared to summertime ($-8.7\,\mu g\,m^{-3}$ vs. $-5.8\,\mu g\,m^{-3}$ respectively for annual average $PM_{2.5}$) due to significant abatement in the heating sector. In contrast, in the Stockholm domain the seasonal and spatial distribution of changes are much less prominent due to the prevailing regional influence (Table 5).

5.4 Future changes in population exposure to ozone

In this section we discuss future changes in SOMO35 over the two study regions. SOMO35 is ozone related population exposure metric recommended by WHO and typically used in health impact assessment studies. SOMO35 is calculated as the sum of the differences between maximum daily 8 h running means and the 70 $\mu g\,m^{-3}$ threshold value.

Present-time levels of SOMO35 in Paris are significantly lower than in the rural areas (represented by the domain average value) due to ozone titration over areas of high NO_x emission. It has been shown already that MD8hr is expected to decline by $\sim 2.5\,\%$ in 2050 (Table 4). Never the less the corresponding drop in SOMO35 is significantly higher reaching 26 % (Table 6) due to the dependence of SOMO35 on its 70 $\mu g\,m^{-3}$ cut-off concentration. In future conditions MD8hr for a considerable number of days will shift below threshold levels substantially reducing SOMO35. Similarly, in the Stockholm city, SOMO35 is expected to drop by 74 % whereas MD8hr by only 17.4 %. The examples of Paris and Stockholm presented here suggest that the use of SOMO35 as an indicator of population exposure may be misleading, since it is based on the underlying hypothesis that no health effects of ozone are present below 70 $\mu g\,m^{-3}$. In the rural areas the implemented emission reduction policies will have substantial benefits in population exposure; SOMO35 drops by 69 % in IdF and by 73 % in the Stockholm domain.

ACPD
15, 27041–27085, 2015

5.5 Future evolution of ozone chemical regimes under local and regional scale chemistry-transport modeling in Paris

In this section we study the long-term evolution of ozone chemical regimes in the city of Paris. This analysis is not performed for Stockholm where ozone concentrations are controlled by long-range transport and less by the local chemistry which determines the regime (see discussion in Sect. 5.3). For each simulated day in the ozone period, in both present and future decades, we determine MD8hr concentrations of NO_y and the ratios of $O_3 : NO_y$, $H_2O_2 : NO_y$ and $H_2O_2 : NO_z$. The threshold values proposed in order to discriminate between the two chemical regimes (i.e., NO_x or VOC-limited) are 7.6 ppb for NO_x (Beekman and Vautard, 2010), 5.5 for $O_3 : NO_y$ (Sillman et al., 2003), 0.12 for $H_2O_2 : NO_y$ (Sillman and He, 2002) and between 0.21 and 0.41 for $H_2O_2 : NO_z$ (Beekman and Vautard, 2010). The aforementioned analysis is applied on both regional (coarse-res) and urban-scale (high-res) simulations for present and future decades. Three indicators agree on a VOC-limited characterization of present-time ozone production at the urban scale simulation in agreement to the findings of Markakis et al. (2014) while only two indicators classify the regional scale ozone simulation as VOC-limited (Fig. 6). Despite a similar trend towards a more NO_x-limited photochemistry in 2050 at both high and coarse simulations, still three out of four indicators characterize the high-resolution simulation as VOC-limited at 2050 whereas the coarse resolution is positively NO_x-limited according to all four indicators.

5.6 Policy implications based on comparison of air quality projections from high and coarse resolution modeling

Air quality projections for 2050 indicate that ozone levels in Paris will increase by 8 and 3 % for daily average and MD8hr respectively as a response to the enforced emission mitigation plan. On the contrary, the coarse resolution simulation yields 7 and 15 % decrease in these metrics (Table 7). A similar inconsistency was found in Markakis et al. (2014), where the Global Energy Assessment (GEA) emission projection (Riahi

ACPD
15, 27041–27085, 2015

et al., 2014) was used instead of the ECLIPSE inventory. ECLIPSE stands as another state-of-the-art emission inventory, explicitly designed for air-quality projections in order to cope with the drawbacks (Butler et al., 2012) of their global counterparts such as the RCPs which were intended for use in global scale climate studies. As discussed in the previous section, ozone production in the coarse resolution simulation by 2050 will shift from a VOC- to a NO_x-limited photochemical regime and therefore more responsive to reductions of NO_x emissions compared to the urban-scale simulation where the transition to NO_x-limited conditions is smoother. PM concentrations over Paris under the high-resolution modeling are expected to decrease by 21 to 46 % depending on the season and particle cut-off diameter while the coarse-resolution simulation is about 10 % more optimistic with reductions ranging from 34 to 55 %. Both the evolution of chemical regimes and of PM concentrations are attached to the underlying emission projections. Under the coarse-scale storyline (CLE), annual emissions of NO_x over Paris drop by almost an order of magnitude while the local inventory yields a reduction of 66 %. Annual PM_{10} and $PM_{2.5}$ emissions in Paris drop by 76 % according to CLE while only by 10 and 38 % respectively according to the local projection.

Given that the coarse inventory implements assessment at the large scale, its stronger mitigation over the city of Paris compared to the AIRPARIF projection is due to omission of local policy. The downscaling of coarse inventories on regional scale CTM grids passes through spatial proxies (such as land-use) to distribute emissions and the related bias induced to the air-quality simulation over finer areas increases the overall bias of the application as well. The difference in the response of the regional and urban scale simulations is due, at large extent, to the spatial allocation algorithm (inherited by the RCPs) used in the compilation of both GEA and ECLIPSE databases (Riahi et al., 2011), which forces stronger (and possibly unrealistic) mitigation over the urban areas. Additionally, regional inventories assimilate regional/national legislation. In Europe the UNECE/LRTAP convention under the revised Gothenburg protocol (http://www.unece.org/fr/env/lrtap/status/lrtap_s.html) bounds the European member states (EU28) to achieve at a 2020 horizon relative to 2005 an overall reduction by 42 %

ACPD
15, 27041–27085, 2015

in NO_x emissions and 28 % in NMVOCs emissions. Such reductions enhance the shift towards NO_x-limited ozone production. This remark, suggests that coarse-resolution ozone projections may be too optimistic over VOC-limited areas, mainly found in North-Western Europe (Beekman and Vautard, 2010) as well as PM projections over heavily populated urban areas. It is plausible that new updated protocols taking into account regional particularities should be implemented in European emission mitigation schemes and more credible assessments could be achieved by incorporating local policy in large scale inventories. This point is particularly relevant for areas such as Stockholm, where the regional scale mainly drives pollutant concentrations. The transfer of bias from the larger to the finer scale may lead to misclassification of local policy.

Despite the large differences in ozone concentrations simulated at regional and urban scales over the urban area of the city of Paris, rural concentrations are very similar; the projections at both scales show a decrease in ozone at 2050 at comparable magnitudes (Table 7). Therefore, fine-scale information provides little advantage in simulating rural ozone responses in agreement with Markakis et al. (2014). On the contrary, PM rural projections are very different between simulations at different resolutions (Table 7) suggesting that regional scale biases may be transferred to the finer scale run.

A final remark relates to the relative role of climate-change and emissions in future pollutant concentration projections. In contrast to the general conclusion of most recent pan-European scale studies (Colette et al., 2013; Geels et al., 2015; Lacressonnière et al., 2014; Watson et al., 2015; Langner et al., 2012b) we find that maximum ozone projections over Paris, modelled at the local scale are more sensitive (based on the absolute concertation change from present day) to climate change than to emission mitigation (Sect. 5.3). This suggests that the coarse-resolution applications could overestimate the magnitude of the contribution of the future emissions mitigation to the overall ozone concentration response.

ACPD
15, 27041–27085, 2015

6 Conclusions

Long-term projections of air quality at the urban scale integrating local emission policies are scarce. In the present study we investigate mid-21st century ozone and particulate matter concentrations focusing on two European cities: Paris, France and Stockholm, Sweden. Using a fine resolution modeling system (4 km for the IdF region and 1 km for Stockholm) we quantify the contribution of emission reduction policies and of climate-change to pollutant concentration changes at the 2050 horizon. For the Stockholm region we distinguish the role of locally enforced mitigation from that of regional-scale changes in emissions (European policy). Local scale emission changes rely on 2030 projections compiled by authorized air-quality agencies at Paris and Stockholm.

The analysis of present-time ozone concentrations reveals very different photochemical conditions in the two case-studies; ozone formation in Paris is characterized as VOC-limited, with ozone titration being the main driver of concentration levels over the city, while both PM and ozone concentrations in Stockholm depend on long-range transport of pollution (96 and 70 % of the local MD8hr and annual PM concentrations respectively originate from non-local sources).

Overall we identify an ozone (daily average and maximum) climate benefit up to −5 % in IdF and −2 % in Stockholm city despite the overall increase in the mean surface temperatures. For IdF this is not related to changes in local titration (as NO_x concentrations are little affected by 2050) but to changes in the regional climate. Provided the dominant regional influence in Stockholm, it is not surprising that the climate change contribution to the final PM concentrations follows the weak trend observed at continental scale simulations. In IdF, PM concentrations are expected to decrease due to the wetter climate predicted for the region although the trend is very weak.

We find that the mitigation of ozone-precursor emissions implemented in the IdF region instigates spatially irregular ozone concentration changes with a benefit over the rural areas (−9 and −12 % for daily average and MD8hr respectively) while, over the urban area we observe a penalty of +8 and +3 % in daily mean and MD8hr ozone

ACPD
15, 27041–27085, 2015

concentrations respectively due to titration inhibition. Under VOC-sensitivity ozone benefit may be attained by either pushing NMVOCs mitigation over NO_x or by enforcing stronger mitigation of NO_x emissions that will allow a shift of the photochemical regime towards NO_x-limited conditions prior to 2050. In our assessment neither is valid. The long-term evolution of chemical regimes studied with the use of regime indicators has shown that the city will not undergo the regime shift by 2050.

In Paris, the increase in the daily average ozone due to emission changes counterbalances the climate benefit to such extend that the combined effect is an overall penalty of +2 %. In contrast changes in MD8hr concentrations due to climate ($\Delta c = -4.1\,\mu g\,m^{-3}$) are larger compared to those introduced by emission abatement ($\Delta c = +2.2\,\mu g\,m^{-3}$), indicating that the local maximum is more sensitive to climate change while background ozone concentration levels are more sensitive to emission changes. In the Stockholm city and the domain, emission mitigation is largely influential, with reductions several times higher than those introduced by climate both for ozone and PM. Contrary to Paris, we show that this response is entirely attributed to changes at the regional scale. Finally, the cumulative effect of climate and emissions in the city of Paris reaches +2.3 % for daily average ozone, −2.4 % for MD8hr ozone, −26 % for SOMO35, −33 % for PM_{10} and −45 % for $PM_{2.5}$ while for the Stockholm city, −17 % for daily average ozone, −18 % for MD8hr ozone, −74 % for SOMO35, −20 % for PM_{10} and −20 % for $PM_{2.5}$.

Another aim of this work was to quantify the plausible added value of the assimilation of local policy into regional scale inventories. To do so, we compared pollutant concentration changes modeled over the two cities at urban scale against regional-scale simulations over the same areas forced by ECLIPSE, a state of the art emission inventory designed to cope with the drawbacks of inventories such as the RCPs, by assimilating air-quality policy at a continental scale. Over Paris the regional scale simulation is more optimistic than its urban scale counterpart. The fine scale modeling yields increase in ozone over the city of Paris (by 8 and 3 % for daily average and MD8hr respectively) while the regional scale modeling yields a 7 and 15 % drop respectively. Regional scale

ACPD
15, 27041–27085, 2015

simulations are more optimistic for PM concentrations as well with about 10 % larger reductions compared to the urban scale projections. These discrepancies are a direct effect of the much stricter mitigation of primary anthropogenic emissions under the ECLIPSE scenario.

Overall our assessment suggests that the long-term evolution of atmospheric pollution solely based on regional scale emissions may lead to misclassification of the effect. The stricter mitigation in ECLIPSE projections is mainly due to the spatial allocation algorithm, which assigns unrealistically high mitigation over urban areas. It is plausible that new updated protocols taking into account the particularities of regions should be implemented in European emission mitigation schemes and that more credible assessments could be achieved by incorporating local policy to those inventories. An effect, overlooked by the coarse scale modeling, is the response of MD8hr ozone, a crucial input of health impact assessment studies: for Paris this metric is more prominent to climate change rather than to emission mitigation.

For Stockholm the comparison of regional and urban scale simulations shows small discrepancies given the major role of long-range transport over the area. This stresses the need to better understand the mechanism of bias propagation across the modeling scales in order to design more successful local-scale strategies.

Acknowledgements. This work was carried out within the ACCEPTED project, which is supported by the ERA-ENVHEALTH network (grant agreement no. 219337), with funding from ANSES, ADEME, BelSPO, UBA and the Swedish EPA. Part of the work was also funded by the European Union Seventh Framework Programme (FP7/2007–2013) under the project 760 IMPACT2C: Quantifying projected impacts under 2 °C warming, grant agreement no. 282746. The ECLIPSE emissions used in this study have been developed by IIASA under the European Commission FP7 project ECLIPSE (Project no. 282688), while additional tasks (development of the MFR scenario) where supported by PEGASOS (Project no. 282688) and "Assessment of hemispheric air pollution on EU air policy" (contract no. 07.0307/2011/605671/SER/C3).

ACPD
15, 27041–27085, 2015

References

AIRPARIF: Evaluation Prospective des emissions et des concentrations des pollutants atmospheriques a l'horizon 2020 en Ile-De-France – Gain sur les emissions en 2015, available at: http://www.airparif.asso.fr/_pdf/publications/ppa-rapport-121119.pdf (last access: 30 September 2015), 2012.

Amann, M., Bertok, I., Borken-Kleefeld, J., Cofala, J., Heyes, C., Höglund-Isaksson, L., Klimont, Z., Nguyen, B., Posch, M., Rafaj, P., Sandler, R., Schöpp, W., Wagner, F., and Winiwarter, W.: Cost-effective control of air quality and greenhouse gases in Europe: modeling and policy applications, Environ. Modell. Softw., 26, 1489–1501, 2011.

Andersson, C., Langner, J., and Bergström, R.: Interannual variation and trends in air pollution over Europe due to climate variability during 1958–2001 simulated with a regional CTM coupled to the ERA40 reanalysis, Tellus B, 59, 77–98, doi:10.1111/j.1600-0889.2006.00196.x, 2007.

Andersson, C. and Engardt, M.: European ozone in a future climate: importance of changes in dry deposition and isoprene emissions, J. Geophys. Res., 115, D02303, doi:10.1029/2008JD011690, 2010.

Andersson, C., Bergström, R., Bennet, C., Robertson, L., Thomas, M., Korhonen, H., Lehtinen, K. E. J., and Kokkola, H.: MATCH–SALSA – Multi-scale Atmospheric Transport and CHemistry model coupled to the SALSA aerosol microphysics model – Part 1: Model description and evaluation, Geosci. Model Dev., 8, 171–189, doi:10.5194/gmd-8-171-2015, 2015.

Aw, J. and Kleeman, M. J.: Evaluating the first-order effect of intra-annual temperature variability on urban air pollution, J. Geophys. Res., 108, 4365, doi:10.1029/2002JD002688, 2003.

Beekmann, M. and Vautard, R.: A modelling study of photochemical regimes over Europe: robustness and variability, Atmos. Chem. Phys., 10, 10067–10084, doi:10.5194/acp-10-10067-2010, 2010.

Bergström, R., Denier van der Gon, H. A. C., Prévôt, A. S. H., Yttri, K. E., and Simpson, D.: Modelling of organic aerosols over Europe (2002–2007) using a volatility basis set (VBS) framework: application of different assumptions regarding the formation of secondary organic aerosol, Atmos. Chem. Phys., 12, 8499–8527, doi:10.5194/acp-12-8499-2012, 2012.

Bergström, R., Hallquist, M., Simpson, D., Wildt, J., and Mentel, T. F.: Biotic stress: a significant contributor to organic aerosol in Europe?, Atmos. Chem. Phys., 14, 13643–13660, doi:10.5194/acp-14-13643-2014, 2014.

ACPD
15, 27041–27085, 2015

Coleman, L., Martin, D., Varghese, S., Jennings, S. G., and O' Dowd, C. D.: Assessment of changing meteorology and emissions on air quality using a regional climate model: impact on ozone, Atmos. Environ., 69, 198–210, 2014.

Colette, A., Granier, C., Hodnebrog, Ø., Jakobs, H., Maurizi, A., Nyiri, A., Rao, S., Amann, M., Bessagnet, B., D'Angiola, A., Gauss, M., Heyes, C., Klimont, Z., Meleux, F., Memmesheimer, M., Mieville, A., Rouïl, L., Russo, F., Schucht, S., Simpson, D., Stordal, F., Tampieri, F., and Vrac, M.: Future air quality in Europe: a multi-model assessment of projected exposure to ozone, Atmos. Chem. Phys., 12, 10613–10630, doi:10.5194/acp-12-10613-2012, 2012.

Colette, A., Bessagnet, B., Vautard, R., Szopa, S., Rao, S., Schucht, S., Klimont, Z., Menut, L., Clain, G., Meleux, F., Curci, G., and Rouïl, L.: European atmosphere in 2050, a regional air quality and climate perspective under CMIP5 scenarios, Atmos. Chem. Phys., 13, 7451–7471, doi:10.5194/acp-13-7451-2013, 2013.

Clarke, L., Edmonds, J., Jacoby, H., Pitcher, H., Reilly, J., and Richels, R: Scenarios of Greenhouse Gas Emissions and Atmospheric Concentrations. Sub-report 2.1A of Synthesis and Assessment Product 2.1 by the US Climate Change Science Program and the Subcommittee on Global Change Research. Department of Energy, Office of Biological and Environmental Research, Washington, 7 D. C., USA, 154 pp., 2007.

Deguillaume, L., Beekmann, M., and Derognat, C.: Uncertainty evaluation of ozone production and its sensitivity to emission changes over the Ile-de-France region during summer periods, J. Geophys. Res., 113, D02304, doi:10.1029/2007JD009081, 2008.

Dufresne, J.-L., Foujols, M.-A., Denvil, S., Caubel, A., Marti, O., Aumont, O., Balkanski, Y., Bekki, S., Bellenger, H., Benshila, R., Bony, S., Bopp, L., Braconnot, P., Brockmann, P., Cadule, P., Cheruy, F., Codron, F., Cozic, A., Cugnet, D., de Noblet, N., Duvel, J.-P Ethé, C., Fairhead, L., Fichefet, T., Flavoni, S., Friedlingstein, P., Grandpeix, J.-Y., Guez, L., Guilyardi, E., Hauglustaine, D., Hourdin, F., Idelkadi, A., Ghattas, J., Joussaume, S., Kageyama, M., Krinner, G., Labetoulle, S., Lahellec, A., Lefebvre, M.-P., Lefevre, F., Levy, C., Li, Z. X., Lloyd, J., Lott, J., Madec, G., Mancip, M., Marchand, M., Masson, S., Meurdesoif, Y., Mignot, J., Musat, I., Parouty, S., Polcher, J., Rio, C., Schulz, M., Swingedouw, D., Szopa, S., Talandier, C., Terray, P., Viovy, N., and Vuichard, N.: Climate change projections using the IPSL-CM5 earth system model: from CMIP3 to CMIP5, Clim. Dynam., 40, 2123–2165, 2013.

ACPD
15, 27041–27085, 2015

Engardt, M., Bergstrom, R., and Andersson, C.: Climate and emission changes contributing to changes in near-surface ozone in Europe over the coming decades: results from model studies, Ambio, 38, 452–458, doi:10.1579/0044-7447-38.8.452, 2009.

Environmental Protection Agency (EEA): Air quality in Europe – 2013 report, available at: http://www.eea.europa.eu/publications/air-quality-in-europe-2013 (last access: 30 September 2015), 2013.

Geels, C., Andersson, C., Hänninen, O., Lansø, A. S., Schwarze, P. E., Skjøth, C. A., and Brandt, J.: future premature mortality due to O_3, secondary inorganic aerosols and primary PM in Europe – sensitivity to changes in climate, anthropogenic emissions, population and building stock, Int. J. Environ. Res. Public Health, 12, 2837–2869, 2015.

Gidhagen, L., Engardt, M., Lövenheim, B., and Johansson, C.: Modeling effects of climate change on air quality and population exposure in urban planning scenarios, Adv. Meteorol., 2012, 240894, doi:10.1155/2012/240894, 2012.

Guenther, A., Karl, T., Harley, P., Wiedinmyer, C., Palmer, P. I., and Geron, C.: Estimates of global terrestrial isoprene emissions using MEGAN (Model of Emissions of Gases and Aerosols from Nature), Atmos. Chem. Phys., 6, 3181–3210, doi:10.5194/acp-6-3181-2006, 2006.

Giorgi, F., Coppola, E., Solmon, F., Mariotti, L., Sylla, M. B., Bi, X., Elguindi, N., Diro, G. T., Nair, V., Giuliani, G., Turuncoglu, U. U., Cozzini, S., Güttler, L., O'Brien, T. A., Tawfik, A. B., Shalaby, A., Zakey, A. S., Steiner, A. L., Stordal, F., Sloan, L. C., and Brankovic, C.: RegCM4: model description and preliminary tests over multiple CORDEX domains, Clim. Res., 52, 7–29, 2012.

Hauglustaine, D. A., Hourdin, F., Jourdain, L., Filiberti, M.-A., Walters, S, Lamarque, J. F., and Holland, E. A.: Interactive chemistry in the laboratoire de meteorologie dynamique general circulation model: description and background tropospheric chemistry evaluation, J. Geophys. Res., 190, D04314, doi:10.1029/2003JD003957, 2004.

Jacob, D. J. and Winner, D. A.: Effect of climate change on air quality, Atmos. Environ., 43, 51–63, 2009.

Jacob, D., Petersen, J., Eggert, B., Alias, A., Christensen, O. B., Bouwer, L. M., Braun, A., Colette, A., Déqué, M., Georgievski, G., Georgopoulou, E., Gobiet, A., Menut, L., Nikulin, G., Haensler, A., Hempelmann, N., Jones, C., Keuler, K., Kovats, S., Kroner, N., Kotlarski, S., Kriegsmann, A., Martin, E., van Meijgaard, E., Moseley, C., Pfeifer, S., Preuschmann, S., Radermacher, C., Radtke, K., Rechid, D., Rounsevell, M., Samuelsson, P., Somot, S., Sous-

ACPD
15, 27041–27085, 2015

sana, J.-F., Teichmann, C., Valentini, R., Vautard, R., Weber, B., and Yiou, P.: EURO-CORDEX: new high-resolution climate change projections for European impact research, Reg. Environ. Change, 14, 563–578, doi:10.1007/s10113-013-0499-2, 2014.

Jerrett, M., Finkelstein, M. M., Brook, J. R., Arain, M. A., Kanaroglou, P., Stieb, D. M., Gilbert, N. L., Verma, D., Finkelstein, N., Chapman, K. R., and Sears, M. R.: A cohort study of traffic-related air pollution and mortality in Toronto, Ontario, Canada, Environ. Health Perspect., 117, 772–777, 2009.

Johnson, C. E., Collins, W. J., Stevenson, D. S., and Derwent, R. G.: The relative roles of climate and emissions changes on future oxidant concentrations, J. Geophys. Res., 104, 18631–18645, 1999.

Kahnert, M.: Variational data analysis of aerosol species in a regional CTM: background error covariance constraint and aerosol optical observation operators, Tellus B, 60, 753–770, 2008.

Katragkou, E., Zanis, P., Kioutsioukis, I., Tegoulias, I., Melas, D., Krüger, B. C., and Coppola, E.: Future climate change impacts on summer surface ozone from regional climate-air quality simulations over Europe, J. Geophys. Res., 116, D22307, doi:10.1029/2011JD015899, 2011.

Ketzel, M., Omstedt, G., and Johansson, C.: Estimation and validation of $PM_{2.5}$/PM_{10} exhaust and non-exhaust emission factors for practical street pollution modeling, Atmos. Environ., 41, 9370–9385, 2007.

Klimont, Z., Kupiainen, K., Heyes, C., Cofala, J., Rafaj, P., Höglund-Isaksson, L., Borken, J., Schöpp, W., Winiwarter, W., Purohit, P., Bertok, I., and Sander, R.: ECLIPSE V4a: global emission data set developed with the GAINS model for the period 2005 to 2050. Key features and principal data sources, available at: http://eccad.sedoo.fr/eccad_extract_interface/JSF/page_login.jsf (last access: 30 September 2015), 2013.

Lacressonnière, G., Peuch, V.-H., Vautard, R., Arteta, J., Déqué, M., Joly, M., Josse, B., Marécal, V., and Saint-Martin, D.: European air quality in the 2030s and 2050s: impacts of global regional emission trends and of climate change, Atmos. Environ., 92, 348–358, 2014.

Lamarque, J.-F., Bond, T. C., Eyring, V., Granier, C., Heil, A., Klimont, Z., Lee, D., Liousse, C., Mieville, A., Owen, B., Schultz, M. G., Shindell, D., Smith, S. J., Stehfest, E., Van Aardenne, J., Cooper, O. R., Kainuma, M., Mahowald, N., McConnell, J. R., Naik, V., Riahi, K., and van Vuuren, D. P.: Historical (1850–2000) gridded anthropogenic and biomass burn-

ACPD
15, 27041–27085, 2015

ing emissions of reactive gases and aerosols: methodology and application, Atmos. Chem. Phys., 10, 7017–7039, doi:10.5194/acp-10-7017-2010, 2010.
Langner, J., Bergström, R., and Pleijel, K.: European Scale Modeling of Sulfur, Oxidised Nitrogen and Photochemical Oxidants. Model Development and Evaluation for the 1994 Growing Season, Swedish Meteorological and Hydrological Institute, RMK No. 82, 71 pp. (with errata), 1998.
Langner, J., Bergström, R., and Foltescu, V.: Impact of climate change on surface ozone and deposition of sulphur and nitrogen in Europe, Atmos. Environ., 39, 1129–1141, 2005.
Langner, J., Engardt, M., Baklanov, A., Christensen, J. H., Gauss, M., Geels, C., Hedegaard, G. B., Nuterman, R., Simpson, D., Soares, J., Sofiev, M., Wind, P., and Zakey, A.: A multi-model study of impacts of climate change on surface ozone in Europe, Atmos. Chem. Phys., 12, 10423–10440, doi:10.5194/acp-12-10423-2012, 2012a.
Langner, J., Engardt, M., and Andersson, C.: European summer surface ozone 1990–2100, Atmos. Chem. Phys., 12, 10097–10105, doi:10.5194/acp-12-10097-2012, 2012b.
Lattuati, M.: Contribution a l'Etude du Bilan de l'Ozone Tropospherique a l'Interface de l'Europe et de l'Atlantique Nord: Modelisation Lagrangienne et Mesures en Altitude, Phd thesis, Universite P. M. Curie, Paris, France, 1997.
Lauwaet, D., Viaene, P., Brisson, E., van Lipzig, N. P. M., van Noije, T., Strunk, A., Van Looy, S., Veldeman, N., Blyth, L., De Ridder, K., and Janssen, S.: The effect of climate change and emission scenarios on ozone concentrations over Belgium: a high-resolution model study for policy support, Atmos. Chem. Phys., 14, 5893–5904, doi:10.5194/acp-14-5893-2014, 2014.
Lepeule, J., Laden, F., Dockery, D., and Schwartz, J.: Chronic exposure to fine particles and mortality: an extended follow-up of the Harvard Six Cities study from 1974 to 2009, Environ. Health Persp., 120, 965–970, 2012.
Liao, H., Chen, W.-T., and Seinfeld, J. H.: Role of climate change in global predictions of future tropospheric ozone and aerosols, J. Geophys. Res., 111, D12304, doi:10.1029/2005JD006852, 2006.
Likhvar, V., Pascal, M., Markakis, K., Colette, A., Hauglustaine, D., Valari, M., Klimont, Z., Medina, S., and Kinney, P.: A multi-scale health impact assessment of air pollution over the 21st century, Sci. Total Environ., 514, 439–449, 2015.
Markakis, K., Valari, M., Colette, A., Sanchez, O., Perrussel, O., Honore, C., Vautard, R., Klimont, Z., and Rao, S.: Air quality in the mid-21st century for the city of Paris under two

ACPD
15, 27041–27085, 2015

climate scenarios; from the regional to local scale, Atmos. Chem. Phys., 14, 7323–7340, doi:10.5194/acp-14-7323-2014, 2014.
Markakis, K., Valari, M., Perrussel, O., Sanchez, O., and Honore, C.: Climate-forced air-quality modeling at the urban scale: sensitivity to model resolution, emissions and meteorology, Atmos. Chem. Phys., 15, 7703–7723, doi:10.5194/acp-15-7703-2015, 2015.
Megaritis, A. G., Fountoukis, C., Charalampidis, P. E., Denier van der Gon, H. A. C., Pilinis, C., and Pandis, S. N.: Linking climate and air quality over Europe: effects of meteorology on $PM_{2.5}$ concentrations, Atmos. Chem. Phys., 14, 10283–10298, doi:10.5194/acp-14-10283-2014, 2014.
Menut, L., Schmechtig, C., and Marticorena, B.: Sensitivity of the sandblasting fluxes calculations to the soil size distribution accuracy, J. Atmos. Ocean. Tech., 22, 1875–1884, 2005.
Menut, L., Bessagnet, B., Khvorostyanov, D., Beekmann, M., Blond, N., Colette, A., Coll, I., Curci, G., Foret, G., Hodzic, A., Mailler, S., Meleux, F., Monge, J.-L., Pison, I., Siour, G., Turquety, S., Valari, M., Vautard, R., and Vivanco, M. G.: CHIMERE 2013: a model for regional atmospheric composition modelling, Geosci. Model Dev., 6, 981–1028, doi:10.5194/gmd-6-981-2013, 2013.
Nenes, A., Pilinis, C., and Pandis, S.: ISORROPIA: A new thermodynamic model for inorganic multicomponent atmospheric aerosols, Aquat. Geochem., 4, 123–152, 1998.
Nolte, C. G., Gilliland, A. B., Hogrefe, C., and Mickley, L. J.: Linking global to regional models to assess future climate impacts on surface ozone levels in the United States, J. Geophys. Res., 113, D14307, doi:10.1029/2007JD008497, 2008.
Omstedt, G., Bringfelt, B., and Johansson, C.: A model for vehicle-induced non-tailpipe emissions of particles along Swedish roads, Atmos. Environ., 39, 6088–6097, 2005.
Pascal, M., Corso, M., Chanel, O., Declecq, C., Badaloni, C., Cesaroni, G., Henschel, S., Maister, K., Haluza, D., Martin-Olmedo, P., and Medina, S.: Assessing the public health impact of urban air pollution in 25 European cities: results of the Aphekom project, Sci. Total Environ., 449, 390–400, 2013.
Prather, M., Gauss, M., Berntsen, T., Isaksen, I., Sundet, J., Bey, I., Brasseur, G., Dentener, F., Derwent, R., Stevenson, D., Grenfell, L., Hauglustaine, D., Horowitz, L., Jacob, D., Mickley, L., Lawrence, M., von Kuhlmann, R., Muller, J.-F., Pitari, G., Rogers, H., Johnson, M., van Weele, M., and Wild, O.: Fresh air in the 21st century?, Geophys. Res. Lett., 30, 1100, doi:10.1029/2002GL016285, 2003.

ACPD
15, 27041–27085, 2015

REVIHAAP: Review of evidence on health aspects of air pollution – REVIHAAP Project, available at: http://www.euro.who.int/en/health-topics/environment-and-health/air-quality/ and publications/2013/review-of-evidence-on-health-aspects-of-air-pollution-revihaap-project-final-technical-report (last access: 30 September 2015), 2013.

Riahi, K., Rao, S., Krey, V., Cho, C., Chirkov, V., Fischer, G., Kindermann, G., Nakicenovic, N., and Rafaj, P.: RCP 8.5-A scenario of comparatively high greenhouse gas emissions, Climatic Change, 109, 33–57, 2011.

Robertson, L., Langner, J., and Engardt, M.: An Eulerian limited-area atmospheric transport model, J. Appl. Meteorol., 38, 190–210, 1999.

Seinfeld, J. H. and Pandis, S. N.: Atmospheric Chemistry and Physics: From Air Pollution to Climate Change, 2nd Edn., John Wiley and Sons, Hoboken, NJ, 2006.

Skamarock, W. C. and Klemp, J. B.: A time-split non-hydrostatic atmospheric model, J. Comput. Phys., 227, 3465–3485, 2008.

Sillman, S. and He, D.: Some theoretical results concerning O_3-NO_x-VOC chemistry and NO_x-VOC indicators, J. Geophys. Res., 107, 4659, doi:10.1029/2001JD001123, 2002.

Sillman, S., Vautard, R., Menut, L., and Kley, D.: O_3-NO_x-VOC sensitivity and NO_x-VOC indicators in Paris: Results from models and atmospheric pollution over the paris area (ESQUIF) measurements, J. Geophys. Res., 108, 8563, doi:10.1029/2002JD001561, 2003.

Simpson, D., Benedictow, A., Berge, H., Bergström, R., Emberson, L. D., Fagerli, H., Flechard, C. R., Hayman, G. D., Gauss, M., Jonson, J. E., Jenkin, M. E., Nyíri, A., Richter, C., Semeena, V. S., Tsyro, S., Tuovinen, J.-P., Valdebenito, Á., and Wind, P.: The EMEP MSC-W chemical transport model – technical description, Atmos. Chem. Phys., 12, 7825–7865, doi:10.5194/acp-12-7825-2012, 2012.

Sjödin, A., Ekström, M., and Hammarström, U.: Implementation and Evaluation of the ARTEMIS Road Model for Sweden's International Reporting Obligations on Air Emissions, in: Proceedings of the 2nd Conference Environment and Transport including the 15th Conference of Transport and Air Pollution, Reims, France, June 2006, Vol. 1, 375–382, 2006.

Strandberg, G., Bärring, L., Hansson, U., Jansson, C., Jones, C., Kjellström, E., Kolax, M., Kupiainen, M., Nikulin, G., Samuelsson, P., Ullerstig, A., and Wang, S.: CORDEX scenarios for Europe from the Rossby Centre regional climate model RCA4, SMHI reports, RMK 116, ISSN 0347–2116, 2014.

ACPD
15, 27041–27085, 2015

Szopa, S. and Hauglustaine, D.: Relative impacts of worldwide tropospheric ozone changes and regional emission modifications on european surface-ozone levels, CR. Geosci., 339, 709–720, 2007.
Szopa, S., Hauglustaine, D. A., Vautard, R., and Menut, L.: Future global tropospheric ozone changes and impact on european air quality, Geophys. Res. Lett., 33, L14805, doi:10.1029/2006GL025860, 2006.
Szopa, S., Balkanski, Y., Schulz, M., Bekki, S., Cugnet, D., Fortems-Cheiney, A., Turquety, S., Cozic, A., Deandreis, C., Hauglustaine, D., Idelkadi, A., Lathiere, J., Lefevre, F., Marchand, M., Vuolo, R., Yan, N., and Dufresne, J.-L.: Aerosol and ozone changes as forcing for climate evolution between 1850 and 2100, Clim. Dynam., 40, 2223–2250, 2013.
Valari, M. and Menut, L.: Does an increase in air quality models' resolution bring surface ozone concentrations closer to reality?, J. Atmos. Ocean. Tech., 25, 1955–1968, 2008.
Vautard, R., Honoré, C., Beekmann, M., and Rouil, L.: Simulation of ozone during the August 2003 heat wave and emission control scenarios, Atmos. Environ., 39, 2957–2967, 2005.
Vautard, R., Builtjes, P. H. J., Thunis, P., Cuvelier, C., Bedogni, M., Bessagnet, B., Honore, C., Moussiopoulos, N., Pirovano, G., Schaap, M., Stern, R., Tarasson, L., and Wind, P.: Evaluation and intercomparison of ozone and PM_{10} simulations by several chemistry transport models over four european cities within the CityDelta project, Atmos. Environ., 41, 173–188, 2007.
Vautard, R., Gobiet, A., Sobolowski, S., Kjellström, E., Stegehuis, A., Watkiss, P., Mendlik. T., Landgren, O., Nikulin, G., Teichmann, C., and Jacob, D.: The european climate under a 2 °C global warming, Environ. Res. Lett., 9, 034006, doi:10.1088/1748-9326/9/3/034006, 2014.
Watson, L., Lacressonnière, G., Gauss, M., Engardt, M., Andersson, C., Josse, B., Marécal, V., Nyiri, A., Sobolowski, S., Siour G., and Vautard, R.: The impact of meteorological forcings on gas phase air pollutants over Europe, Atmos. Environ., 119, 240–257, 2015.
Zanis, P., Katragkou, E., Tegoulias, I., Poupkou, A., Melas, D., Huszar, P., and Giorgi, F.: Evaluation of near surface ozone in air quality simulations forced by a regional climate model over Europe for the period 1991–2000, Atmos. Environ., 45, 6489–6500, 2011.

ACPD
15, 27041–27085, 2015

Table 1. Models (and their implemented resolutions) used for the simulations over the study regions.

	Climate		Air-quality	
	IdF	Stockholm	IdF	Stockholm
Global	IPSL-CM5A-MR 1.25° × 1.25°	EC-EARTH 1.125° × 1.25°	LMDz-OR-INCA 3.75° × 1.9°	
Regional	WRF, 0.11°	RCA4, 0.11°	CHIMERE, 0.44°	MATCH, 0.44°/0.11°
Urban	Same as regional	Same as regional	CHIMERE, 4 km	MATCH, 1 km

ACPD
15, 27041–27085, 2015

Table 2. Quantification of the regional and local contributions to the present-time concentration levels at the city of Stockholm.

	City concentration levels ($\mu g\,m^{-3}$)[a]	Local contribution[b]	Regional contribution[c]
Ozone daily mean	62.5	−0.8	63.3
Ozone MD8hr	78.5	−3.3	81.8
PM_{10} annual mean	14.7	5.7	9.0
PM_{10} JJA mean	13.1	3.5	9.6
PM_{10} DJF mean	12.7	4.4	8.3
$PM_{2.5}$ annual mean	7.3	1.9	5.4
$PM_{2.5}$ JJA mean	6.5	1.5	5.0
$PM_{2.5}$ DJF mean	7.7	2.0	5.7

[a] based on the only available urban background station in the domain (Torkel Knutsson).
[b] Calculated from the concentration difference between the Torkel Knutsson and the Norr Malma sites.
[c] Based on measured concentrations at the Norr Malma site.

ACPD
15, 27041–27085, 2015

Table 3. Future changes in key meteorological variables in the study regions under the RCP-4.5 climate scenario. Seasonal averages include both day-time and night-time values.

IdF	Summer (JJA)		Winter (DJF)	
Variable	REF	2050	REF	2050
2 m temperature (°C)	18.8	+0.2	4.2	+0.4
Specific humidity ($g\,kg^{-1}$)	7.9	+0.3	3.4	+0.2
Precipitation ($kg\,m^{-2}$)	118	+7.1	130	+4.7
Radiation ($W\,m^{-2}$)	262	−6.5	50	−1.9
10 m wind speed ($m\,s^{-1}$)	4.0	+0.2	6.8	−0.2
Boundary layer height (m)	643	+22	727	−41
Stockholm domain	**Summer (JJA)**		**Winter (DJF)**	
Variable	REF	2050	REF	2050
2 m temperature (°C)	12.9	+1.3	−1.2	+1.4
Specific humidity ($g\,kg^{-1}$)	7.7	+0.6	3.1	+0.3
Precipitation ($kg\,m^{-2}$)	223	−14	159	+2.7
Radiation ($W\,m^{-2}$)	232	−0.4	28.2	−0.7
10 m wind speed ($m\,s^{-1}$)	3.2	−0.1	4.3	−0.1
Boundary layer height (m)	673	+6	574	−11

ACPD
15, 27041–27085, 2015

Table 4. Changes in pollutants concentrations (in $\mu g\,m^{-3}$) between present (REF) and 2050 for the IdF and Stockholm regions due to climate change, emission reduction policies and their combined effect. Results are presented separately for the urban centres (Paris and Stockholm cities) and the domain averages. Ozone is averaged over the April–August period.

	Ozone		PM_{10}			$PM_{2.5}$		
Paris	mean	MD8hr	JJA	DJF	annual	JJA	DJF	annual
REF	60	79	22	25	25	15	19	18
clim.	−3.3	−4.1	−1.1	+0.6	−1.1	−1.5	+0.1	−1.2
emiss.	+4.8	+2.2	−4.7	−8.1	−7.2	−5.8	−8.7	−8.1
clim. + emiss.	+1.5	−1.9	−5.8	−7.5	−8.3	−7.3	−8.6	−9.3
IdF Domain	mean	MD8hr	JJA	DJF	annual	JJA	DJF	annual
REF	73	92	22	21	23	14	14	15
clim.	−3.7	−4.2	+0.2	−0.2	−0.7	−1.0	0.0	−1.0
emiss.	−6.5	−11.4	−4.0	−6.6	−6.3	−4.1	−6.0	−5.9
clim. + emiss.	−10.2	−15.6	−3.8	−6.8	−7.0	−5.1	−6.0	−6.9
Stockholm	mean	MD8hr	JJA	DJF	annual	JJA	DJF	annual
REF	72	81	7	12	10	5.3	10	7.4
clim.	−1.3	−1.7	+0.1	−0.4	0.0	0.0	−0.3	0.0
emiss.	−11	−12.7	−1.3	−2.2	−2.0	−1.0	−1.8	−1.6
clim. + emiss.	−12.3	−14.4	−1.2	−2.6	−2.0	−1.0	−2.1	−1.6
Stockholm domain	mean	MD8hr	JJA	DJF	annual	JJA	DJF	annual
REF	73	81.5	6.6	11	9	5	9.5	7
clim.	−1.3	−1.1	+0.1	−0.3	+0.1	0.0	−0.3	0.0
emiss.	−11.4	−13.1	−1.3	−2.3	−1.9	−1.0	−1.9	−1.6
clim. + emiss.	−12.7	−14.2	−1.2	−2.6	−1.8	−1.0	−2.2	−1.6

ACPD
15, 27041–27085, 2015

Table 5. Contribution of the emission reduction policies implemented at the local and regional scale to the future concentration changes of ozone, PM_{10} and $PM_{2.5}$ in the Stockholm domain.

	Ozone		PM_{10}			$PM_{2.5}$		
Stockholm domain	mean	MD8hr	JJA	DJF	annual	JJA	DJF	annual
REF	73	81.5	6.6	11	9	5	9.5	7
local	+0.1	+0.1	−0.1	−0.1	−0.1	0.0	0.0	0.0
regional	−11.5	−13.2	−1.2	−2.4	−1.8	−1.0	−1.9	−1.6
local + regional	−11.4	−13.1	−1.3	−2.3	−1.9	−1.0	−1.9	−1.6

ACPD
15, 27041–27085, 2015

Table 6. SOMO35 (in $\mu g\,m^{-3}$ days) in the two study regions for the present day simulation (REF) and the future projection (accounting for both climate and emission changes). The relative change between present and future is also given in parenthesis.

	REF	2050
Paris	9807	7080 (−26 %)
IdF Domain	20 611	7297 (−65 %)
Stockholm	2576	676 (−74 %)
Stockholm Domain	2660	714 (−73 %)

ACPD
15, 27041–27085, 2015

Table 7. Future concentration response relative to present (in %) under the high and coarse-resolution applications over the city of Paris and the IdF domain.

	Ozone		PM_{10}			$PM_{2.5}$		
	mean	MD8hr	JJA	DJF	annual	JJA	DJF	annual
Paris high-res	+8	+3	−21	−32	−32	−38	−46	−44
Paris coarse-res	−7	−15	−34	−47	−42	−43	−55	−52
IdF high-res	−9	−12	−18	−32	−27	−29	−42	−39
IdF coarse-res	−9	−16	−29	−41	−37	−39	−52	−49

ACPD
15, 27041–27085, 2015

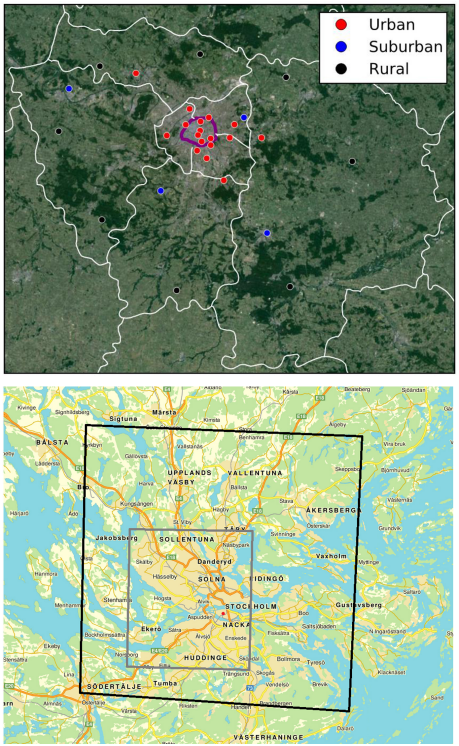

Figure 1. Top panel illustrates the IdF 4 km resolution modeling domain, with the city of Paris in the centre (area enclosed by the purple line). Circles correspond to sites of the local air-quality monitoring network (AIRPARIF) with red for urban, blue for suburban and black for rural. Bottom panel represents the Stockholm 1 km resolution modeling domain (black outline) with the urban area enclosed in the grey rectangle. The red circle corresponds to the urban monitoring

ACPD
15, 27041–27085, 2015

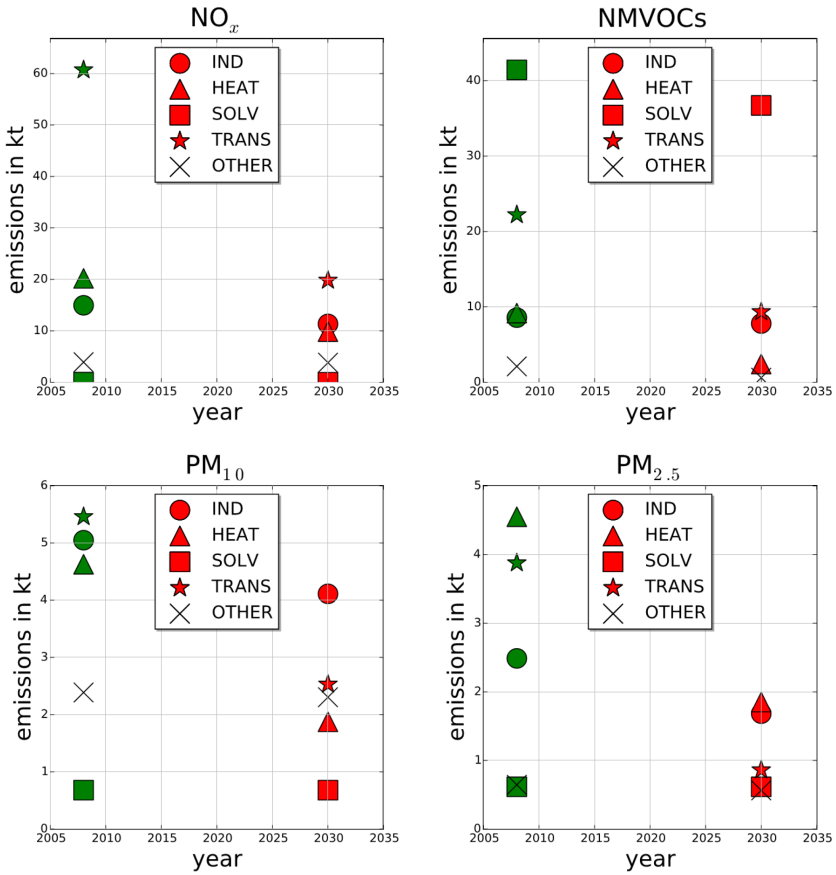

Figure 2. Annual present-time emissions of NO_x, NMVOCs, PM_{10} and $PM_{2.5}$ in IdF and their projections for 2030. IND corresponds to industrial emissions (SNAP1, 3 and 4), HEAT to heating activities (SNAP2), SOLV to solvents use (SNAP6), TRANS to road and non-road transport (SNAP7 and 8) and OTHER represent the remaining source sectors (SNAP5, 9 and 10).

ACPD
15, 27041–27085, 2015

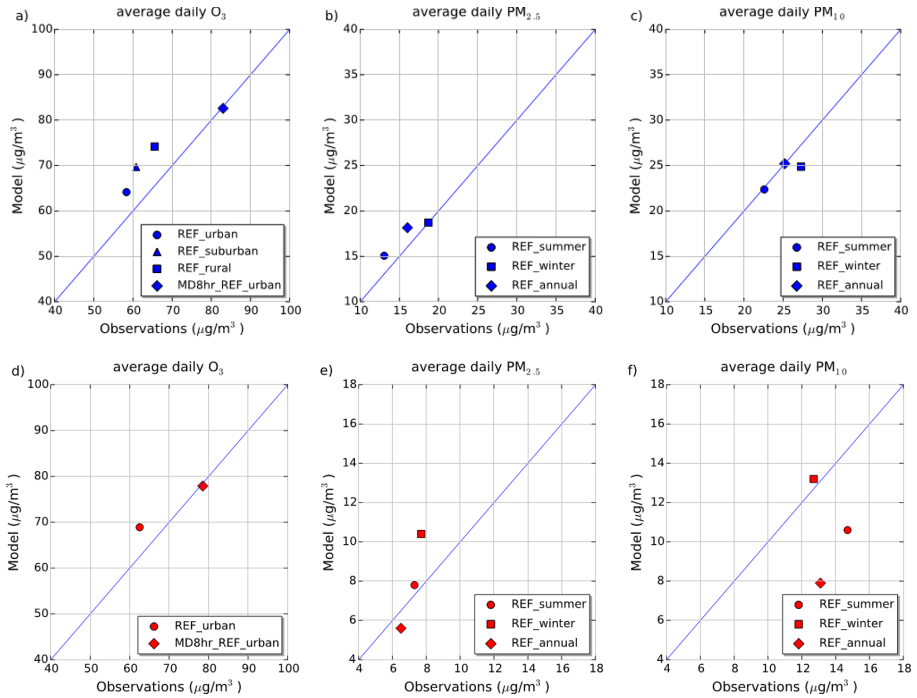

Figure 3. Ozone period (April–August) average ozone concentrations at urban, suburban and rural stations in IdF **(a)** and one urban station in the Stockholm area **(d)**. The average daily maximum 8 h mean values at urban locations are also shown (MD8hr_REF_urban). Average $PM_{2.5}$ and PM_{10} concentrations in wintertime (DJF), summertime (JJA) and on annual basis over urban stations in IdF are shown in panels **(b)**, **(c)** (panels **e**, **f** for Stockholm).

ACPD
15, 27041–27085, 2015

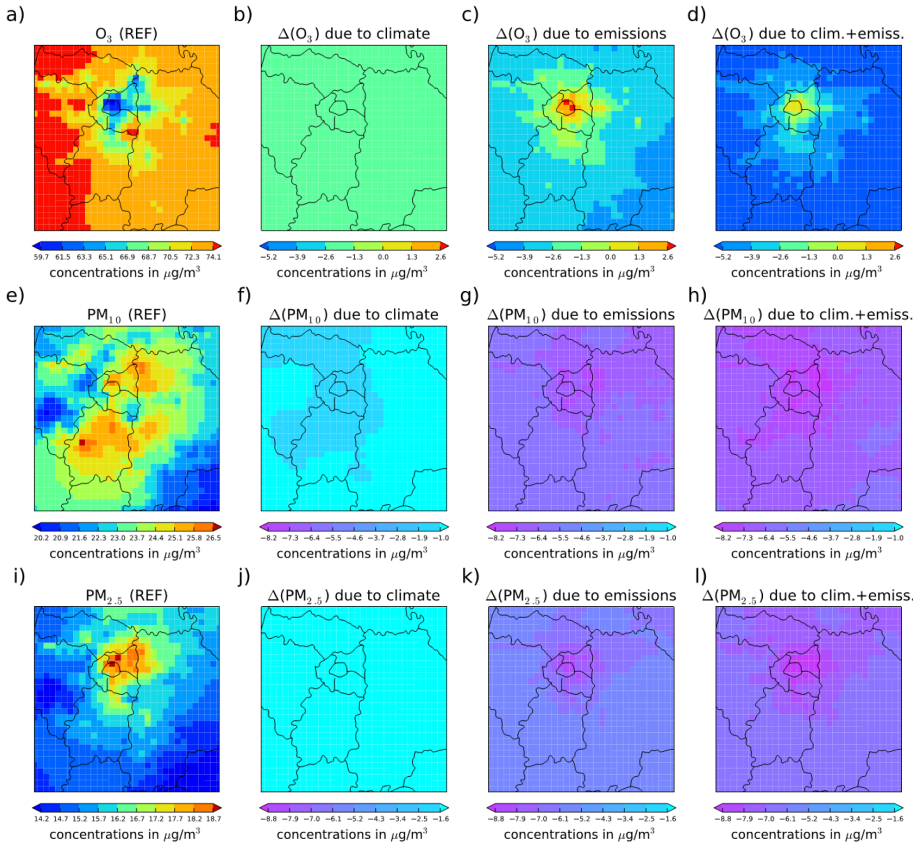

Figure 4. April–August mean ozone, annual mean PM_{10} and annual mean $PM_{2.5}$ concentration maps ($\mu g\,m^3$) for IdF, expressed as absolute values at present-time **(a, e, i)** and as deltas between present-time and 2050 due to climate change **(b, f, j)**, emissions changes **(c, g, k)** and the cumulative effect **(d, h, l)**.

ACPD
15, 27041–27085, 2015

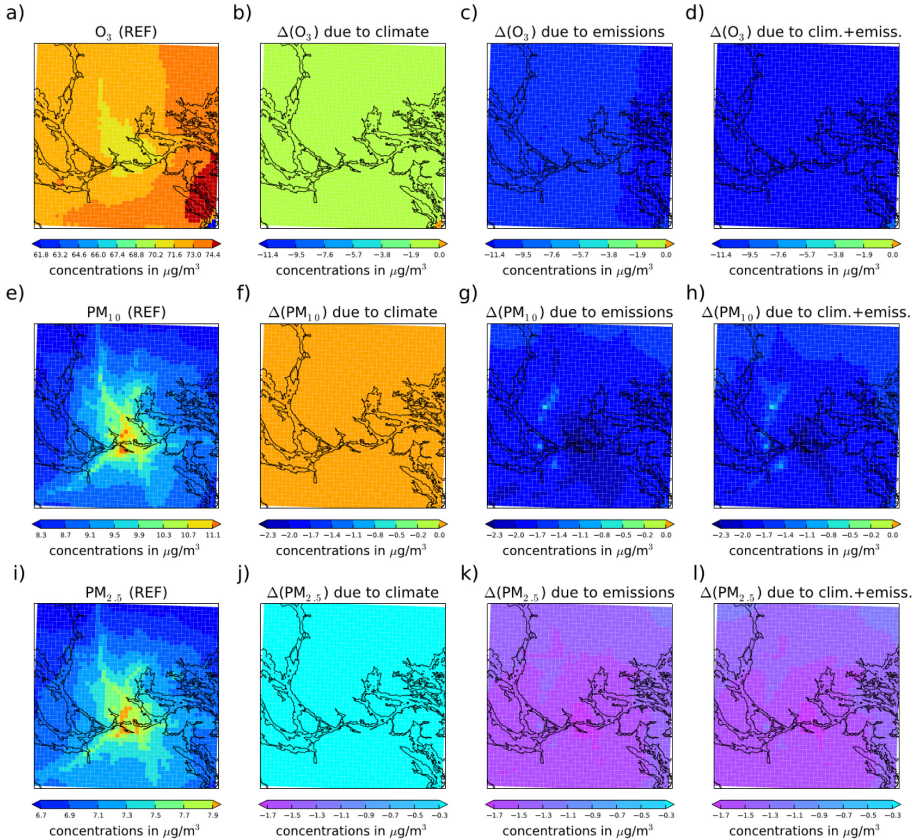

Figure 5. Similar to Fig. 4 for Stockholm.

ACPD
15, 27041–27085, 2015

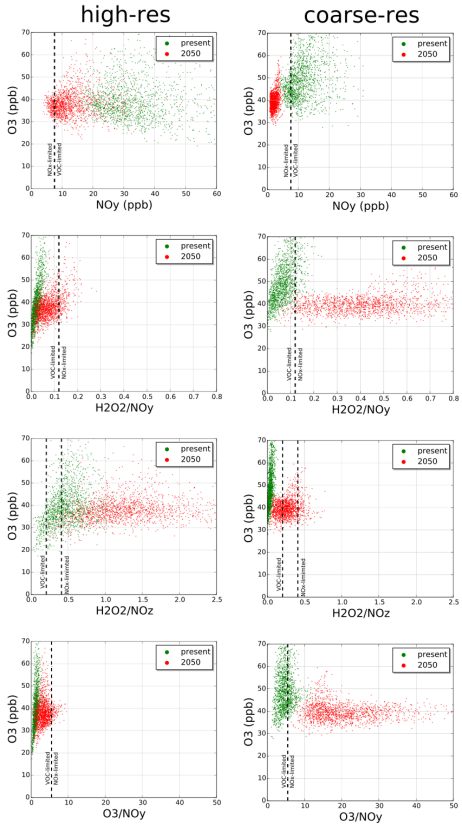

Figure 6. Scatter plots of MD8hr ozone concentrations (y axis) against chemical regime indicators (x axis) for the present and future runs in Paris. Results are presented for the high-resolution (left panels) and the coarse-resolution (right panels) applications. Dots represent MD8hr concentrations for each day of the ozone period. For each indicator the limit value that separates the regimes is also depicted with a dashed line.

ACPD
15, 27041–27085, 2015